



بِسْمِ اللَّهِ الرَّحْمَنِ الرَّحِيمِ
إِنَّا نَسْتَعِينُكَ يَا رَبَّنَا



Sudan University of Science and Technology

College of Engineering

Aeronautical Engineering Department

Design of Electronic Gyroscope

A Thesis Submitted in Partial fulfillment for the Requirements of the Degree
of B.Sc (Honors) in Aeronautical Engineering

Prepared by:

Abuagla omer Al-Amin Ahmed

Ahmed babeker talha Mohammed

Alageba Alshazli Mohammed Salih

Mohamed Hamza Abed almageed Ahmed

Taqwa abd-elwahaab

Supervisor:

Dr. Osman imam

October 2015

[الإستهملال

الآية



سورة الحديد الايه (٩) .

Acknowledgmen

Our acknowledgment and gratefulness at the beginning is to god who gives us the gift mind profound thanks and gratitude to everyone who encourages and support us to complete thisresearch.

Our graduate to our supervisor Dr. Osman Imam.

Also our special thanks for our teachers in aeronautical engineering department .

Also our depth gratitude and special appreciation extended to our friends who stand beside us in every moment.

At the end our gratitude to everyone who help us.



Dedication

This thesis is dedicated to:

Our lovely parents .

Our supervisor Dr. Osman Imam.

Our teachers .

Our friends .



Abstract

This thesis presents a micro electromechanical system-inter digital transducer (MEMS-IDT) surface acoustic wave (SAW) gyroscope with an 80MHz central frequency on a 128° YX lithium-Niobium tri-oxide (LiNbO₃) wafer. The developed MEMS-IDT gyroscope is composed of a two-port SAW resonator, a dual delay line oscillator, and metallic dots. The SAW resonator provides a stable standing wave, and the vibrating metallic dot at an anti node of the standing wave induces the second SAW in the normal direction of its vibrating axis. The dual delay line oscillator detects the Coriolis effect (gyro phenomena) by comparing the resonant frequencies between two oscillators through the interference effect. The coupling of k-wave MATLAB added tool box modeling was used to extract the optimal design parameters prior to simulation. In the electrical testing by the network analyzer, the simulated SAW resonator and delay lines showed low insertion loss and similar operation frequencies between a resonator and delay lines. When the device was rotated, the resonant frequency differences between two oscillators linearly varied owing to the Coriolis force. The obtained sensitivity was approximately 119 Hz deg⁻¹ in the angular rate range of 0-1000deg s⁻¹. Satisfactory linearity and superior directivity were also observed in the test.

Table of Contents

الاستهلال	II
Dedication	III
Acknowledgement	IV
Abstract	V
Table of Contents	VI
List of Figures	IX
List of Symbols	X
Abbreviations	XI

Chapter One: Introduction

1.1 Overview.....	2
1.2 Gyroscopes have two basic properties	2
1.3 Disadvantages of mechanical gyroscope summed up in the following point.....	2
1.4 Digital gyro (MEMS)	3
1.4.1 Effect SAW in MEMS	3
1.5 Problem Statement	4
1.6 proposal solution	4
1.7 Objectives	4
1.8 Motivations.....	4
1.9 Contribution.....	4
1.10 Methodologies	5
1.11 Work Schedule	5

Chapter Two: Literature review

Literature overview.....	7
--------------------------	---

Chapter Three: Mechanical Gyroscope

3.1 Definition of Gyroscope	11
3.2 Principle of Mechanical Gyroscopes	11
3.3 Properties of Mechanical Gyroscopes	11
3.3.1 Rigidity	12
3.3.2 Precession.....	12
3.4 Error of gyro	14
3.4.1 Three General Sources of Mechanical Drift.....	14
3.5 Disadvantages of mechanical gyro.....	15

Chapter Four: Surface acoustic wave

4.1 Surface Acoustic Wave Sensor Definition	17
4.2 SAW types	19
4.3 Operation.....	21
4.4 SAW sensors advantages.....	22
4.5 Application areas	22

Chapter Five: Design of Micro Electrical Mechanical system

5.1 Design Consideration	28
5.1.1 Two-port SAW resonator	28
5.1.2 Metallic dot array.....	29
5.1.3 SAW delay line.....	29
5.2 k-wave Simulation.....	31

Chapter Six: Simulation

6.1 curves of response	33
------------------------------	----

Chapter Seven: Conclusion and Recommendation

7.1 Conclusion.....	36
7.2 Recommendation.....	36

References	38
-------------------------	----

Appendices

Appendix A: Equation of Motion

Appendix B: MATLAB Code

List of Figures

Figure 1 (3-1a) Gyro action.....	13
Figure 2 (3-1b) Gyro action.....	13
Figure 3 (4.1) the basic structure of a SAW device.....	19
Figure 4 (4.2) delay line saw sensor.....	20
Figure 5 (4.3) One-port SAW resonator.....	20
Figure 6 (5.1a). Schematic views and working principle of the SAW gyro scope Entire view of the SAW gyroscope.....	26
Figure 7 (5.1b) Schematic views and working principle of the SAW gyro scope working principle	27
Figure 8 (5.2) (a) Configuration of two-port SAW resonator and (b) the P matrices for the elements of the resonator	30
Figure 9 (5-3) Design of metallic dot array	30
Figure 10 Response of mechanical Gyro.....	33
figure 11 Responseof MEMS Gyro.....	34

List of symbols:

\bar{H}	Is moment of momentum.
J	Torque
$\bar{\omega}$	Angular velocity
\bar{M}	Is a disturbing torque
v_p	Phase velocity
P	pitch
f_s	Synchronize frequency
f_{coriolis}	Force acts on vibrating metallic dots
M	Mass of metallic dot
v	Vibration velocity of the dot
Ω	Rotational velocity of substrate
K	High electromechanical coupling coefficient
λ	Wave length
u_m	Mean velocity in the gab
u_p	Plate velocity

Abbreviations:

MEMS	Micro Electronic Mechanical system
SAW	Surface acoustic waves
IDT	Interdigital transducer
RF	Radio frequency
LiNbO ₃	Lithium niobium tri-oxide
SPUDT	single phase unidirectional transducer
SAWS	Surface acoustic waves used in sensor
SAWF	Surface acoustic waves used in reference

Chapter One

Chapter one

Introduction

1.1 Overview

The word gyroscope was first coined by a French scientist, Leon Foucault, in 1852. It is derived from the Greek words "gyro," a gyroscope is an instrument that maintains an angular reference by virtue of a rapidly spinning, a homogeneous symmetrical heavy mass, rotating about the instantaneous center of mass; all applications of the gyroscope depend on a special form of Newton's second law, which states that a massive, rapidly spinning body rigidly resists being disturbed and tends to react to a disturbing torque by precessing (rotating slowly) in a direction at right angles to the direction of torque.

1.2 Gyroscopes have two basic properties

- Rigidity — the axis of rotation (spin axis) of the gyro wheel tends to remain in a fixed direction in space if no force is applied to it.
- Precession — the axis of rotation has a tendency to turn at a right angle to the direction of an applied force

1.3 Disadvantages of mechanical gyroscope summed up in the following point:

- High cost
- Vibration
- Large weight and volume
- Mechanical drift
- Difficulty of maintenance

1.4 Digital gyro (MEMS)

Micro-Electro-Mechanical-Systems (MEMS) gyroscopes are of the rate measuring type and are typically employed for motion detection (for example, in consumer electronics and automotive safety devices) and motion stabilization and control (for example, in smart automotive steering and antenna/camera stabilization systems).

1.4.1 Effect SAW in MEMS

This review gives an overview of the development of surface acoustic wave (SAW) based gyroscopes. Different types of saw based gyroscope are first presented, which are categorized into standing-wave based or progressive-wave based gyroscopes according to their respective mechanisms. In addition, multi-axis detectable saw based gyroscopes are also introduced in this review. Different principles, structures, production methods, and control technologies are analyzed.

The surface acoustic wave gyroscope was proposed by Lao in 1980. Several research groups have worked on this concept, and a number of related studies were published between 2000 and 2011. SAW gyroscopes detect a change in SAW velocity as a function of the angular rate of the medium in which the SAW propagates. When radio frequency (RF) power supply to inter digital transducers (IDT) is deposited on the surface of a piezoelectric (physical phenomena which convert the stress to electrical) substrate, the IDT generates a SAW. The change in saw velocity due to rotation is then detected as a phase shift between the generated and detected wave velocities. In comparison with conventional MEMS gyroscopes, saw gyroscopes are very attractive for these reasons. As opposed to the MEMS gyroscope, the SAW gyroscope does not need a suspended vibrating mechanical structure. Therefore, it is more resistant to external shocks and vibrations. Frequency matching between the drive and sense-mode frequencies in the absence of active tuning and feedback control is very easy to achieve. Finally, temperature effects that cause variations in the young's modulus and residual stress can be almost completely eliminated easily. In this review, an overview of the development of SAW based gyroscopes is provided. According to their functional principles, SAW gyroscopes are categorized

into different types such as standing-wave-mode type gyroscopes, progressive-wave-mode type gyroscopes, and multi-axis detectable saw gyroscopes, all of which are introduced in this article.

1.5 Problem Statement

Mechanical drifts are inherited problem in mechanical gyro which could not be solved by normal way.

1.6 Proposed Solution

Design of an electronic gyro based on Micro-electro mechanical systems (MEMS) which has the potential of providing reference solution with low cost and hyper sensitivity

1.7 Objective

Design electronics gyroscope to replace the mechanical gyro.

1.8 Motivations

MEMS is most suitable emerging field for Nano technologies .Nano technologies is mostly based on embedded systems so it's an emerging field that motivated us to do this work ,for example: in autopilot, they offer high performance; their performance makes them ideal for safety – critical and time sensitive and their small size make them easy to incorporate into system.

1.9 Contribution

Any mechanical device could replace by a MEMS system.

1.10 Methodologies

Theoretical, analytical, mathematical and software simulation (MATLAB K-wave tool) are applied in this research.

1.11 Work Schedule

This design consisted of seven chapters

- Chapter one is an introduction; which includes: general information of gyroscope, its characteristics, installation, as well as problem of study, objective and significance, the reason why we had done this study and how we work into it.
- Chapter two includes a comprehensive literature review
- Chapter three includes mechanical gyroscope which includes; its concept, formation, and equations of motion, characteristics, as well as effects of drift and its disadvantage.
- Chapter four includes surface acoustic waves (SAW), transuding and piezoelectric material in converting the stress into digital.
- Chapter five includes the main body of design electronic gyroscope.
- Chapter six includes results of analytical and mathematical in a form of simulation diagram by use of MATLAB program.
- Finally chapter seven which include conclusion and recommendation

Chapter Two

Chapter two

Literature review

Surface acoustic wave (SAW) gyroscope was proposed by LAO in 1980 , several research groups have worked on this concept, and a number of related studies were published between 2000 and 2011. SAW gyroscopes detect a change in SAW velocity as a function of the angular rate of the medium in which the SAW propagates. When an RF power supply to inter digital transducers (IDT) is deposited on the surface of a piezoelectric substrate, the IDT generates a SAW. The change in SAW velocity due to rotation is then detected as a phase shift between the generated and detected wave velocities. In comparison with conventional MEMS gyroscopes, SAW gyroscopes are very attractive for these reasons. As opposed to the MEMS gyroscope, the SAW gyroscope does not need a suspended vibrating mechanical structure. Therefore, it is more resistant to external shocks and vibrations. Frequency matching between the drive- and sense-mode frequencies in the absence of active tuning and feedback control is very easy to achieve. Finally, temperature effects that cause variations in the Young's modulus and residual stress can be almost completely eliminated easily. In this review, an overview of the development of SAW based gyroscopes is provided. According to their functional principles, SAW gyroscopes are categorized into different types such as standing-wave-mode type gyroscopes, progressive -wave- mode type gyroscopes, and multi-axis detectable SAW gyroscopes, all of which are introduced in this article. Gyroscopes based on SAW have been reviewed by HAEKWAN OH from AJOU University in 2007 and 2013. In comparison to existing silicon-based MEMS gyroscopes, a SAW gyroscope is very attractive for a number of reasons. First, it has no suspended vibrating mechanical structure and is therefore more resistant to external shocks and vibrations. Second, frequency matching between the drive and sense-mode frequencies in the absence of active tuning and feedback control is very easy. Finally, the temperature effect that causes a variation in the Young's modulus and residual stress can be almost completely eliminated. By comparing different structures of SAW-based gyroscopes and their mechanisms, we can see that the SAW gyroscope has the potential to be the highest performing gyroscope in the near future[1].

The Tiffany Warrington and Eric Wong aimed at characterizing both MEMS accelerometers and gyroscopes for use in a low cost inertial navigation unit. A hardware and software system, consisting of MEMS sensors, A/D converters, a 200 MHz processor, compact flash memory, and C++ coded software, was integrated into a test bed that calculates and outputs the unit's final positioning after acceleration and/or rotation was applied. Testing of the unit proved that low cost sensors, performing at specifications are unable to provide accurate positioning with the current performance of MEMS technology. These tests conclude that these sensors although they do perform according to most of their specifications, are not able to produce accurate results in an inertial navigation system. A more accurate method for determining the bias of the sensors is needed. This would lead to more accurate positioning since the system would be able to determine whether acceleration is positive or negative based on a precise bias. A method for determining when the system is stationary would also be extremely useful. With the high noise that is currently being measured it is difficult for the system to conclude when it is stationary. One method to determine zero movement is through user intervention. When the user knows the system is stationary they could press a button alerting the system to recalibrate. With the current technology in MEMS accelerometers and gyroscopes, it is impossible to create an inertial navigation unit solely dependent on these sensors. The accuracy needed by a firefighter location device is much smaller than the amount that the current sensors can produce. They can be used in conjunction with different technologies such as GPS or digital compasses. For future analysis of the MEMS sensors, it would require a processor that can gather data at a faster rate. Currently taking data at 6 samples per second is not fast enough to do much filtering to distinguish between noise and actual sensor information. Tiffany and Eric project provided a great introduction to the use of low cost MEMS technology in inertial navigation. The final deliverables include an inertial measurement unit that uses a two-axis accelerometer and a gyroscope. The system is capable of storing the data from the sensors and processing it to calculate the final positioning. It was also designed to be compatible with any accelerometer and gyroscope with an analog output. Although the accuracy was less than ideal due to reasons explained earlier, this project was beneficial to gain insight into the developing MEMS technology [2].

Chapter Three

Chapter three

Mechanical Gyroscope

3.1 Definition of Gyroscope

An electro-mechanic device from which angular velocities and displacement could be measured. It consists of a spinning mass, typically a disk or wheel, usually mounted on a gimbal so that its axis can turn freely in one or more directions and thereby maintain its orientation regardless of any movement of the base.

3.2 Principle of Mechanical Gyroscope

When the mass (homogeneous) rotates about its instantaneous axis of rotation, it generates a vector which is constant in the space (inertial space (Newtonian space)).

$$\vec{H} = J \vec{\omega}_{\text{total}} \quad (3-1)$$

3.3 Properties of Mechanical Gyroscopes

Gyroscopes have two basic properties: rigidity and precession. Those properties are defined as follows:

- **RIGIDITY** — the axis of rotation (spin axis) of the gyro wheel tends to remain in a fixed direction in space if no force is applied to it.

$$\vec{H} = \text{const} \quad (3-2)$$

- **PRECESSION** — the axis of rotation has a tendency to turn at a right angle to the direction of an applied force.

$$\vec{M}_{\text{total}} = \frac{d\vec{H}}{dt} \quad (3-3)$$

3.3.1 Rigidity

A fixed direction on Earth is by no means fixed in space, because the Earth turns once on its axis every 24 hours, and makes a complete revolution around the sun every year. The sun itself is moving through space, taking the Earth and the other planets with it. Because of these motions, the expression "fixed direction in space" as used in this explanation is theoretical. For all practical purposes, a line from the Earth to a distant star is a fixed direction in space. If the spin axis of a spinning gyro is pointed at a distant star, it will remain pointed at the star as the Earth turns.

Gyro rigidity is the strength with which a gyro resists any external force that would tilt its rotor spin axis. There are three factors that determine gyro rigidity: weight of the rotor, distribution of this weight, and rotor speed.

The gyro can be considered as an enclosed mechanical system. The energy in the system is equal to the input energy. Hence the energy necessary to spin the gyro rotor is contained in the rotor as angular momentum, which is a function of rotor weight and the speed of rotor rotation. The heavier the gyro rotor, the larger the torque necessary to spin it, and the greater the angular momentum of the rotor. If we have two rotors with identical shapes but different weights spinning at the same velocity, the heavier of the two will be more rigid in its spin axis since it has the greater angular momentum.

3.3.2 Precession

To provide useful information, a gyro's spin axis must be related to some reference, usually the Earth's surface. This is done by using the second fundamental property of a gyro precession. The gyro is processed until its spin axis is pointed in the desired direction. So far we have covered precession in very general terms. The following paragraphs will cover this "gyro action" in more detail. We can show precession by using the models in figure 1 and 2, view (A) and view (B). The gyro wheel is mounted so it is free to have its spin axis pointed in any direction. Here the wheel rotates in a flat loop called the gyro case (inner gimbals). The gyro case is pivoted in the gimbals ring (outer gimbals) and the gyro can swing about the Z axis. The gimbals ring itself turns on pivots that connect it to the fork (support). The fork permits the gyro to tilt from side to side about the Y axis.

Equation of motion of mechanical gyro is attached in appendix A.

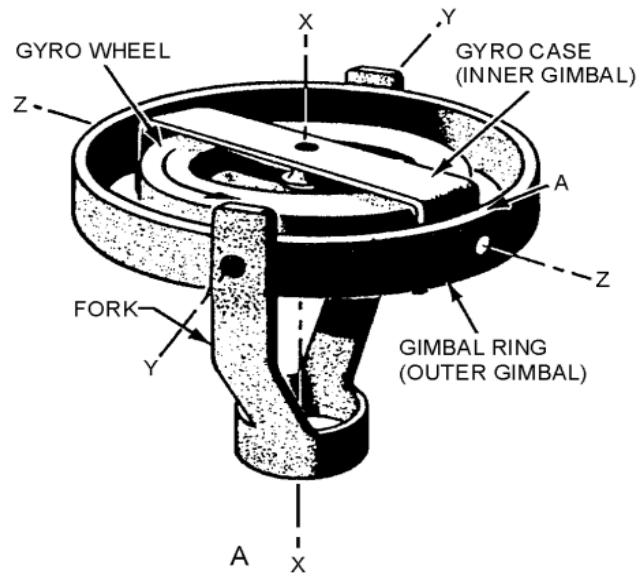


Figure 1 (3-1A)

Gyro action

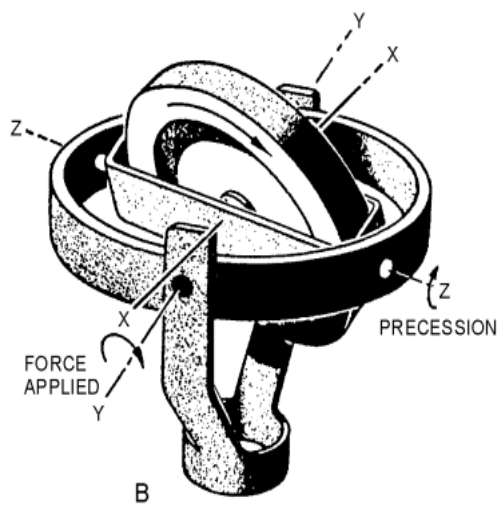


Figure 2 (3-1B)

Gyro action.

Regardless of how the fork is placed, the spinning gyro wheel is free to lie in any given plane. That's why it is called a free gyroscope in this type of mounting. To

show the effect of precession, we can push down on the gimbals ring at point A at the nearer end of the Z-Z axis. You might expect the ring to tilt around the Y-Y axis. Instead, the gyro case will tilt about the Z-Z axis. You can see the effect of this precession in view B.

In the same direction in which the applied force is pushing. Here's a rule that applies to all spinning gyros: (the gyro will always process at right angles to the direction of the applied force). Look at view A again. If we keep pushing down on the gimbals ring at point (A), the gyro case will keep turning until the spin axis of the gyro wheel is horizontal. Then there will be no further precession. At this point the gyro wheel will be spinning.

The motions of a gyroscope can be analyzed according to three basic quantities:

SPIN (the angular velocity of the gyro rotor). TORQUE (the rotary motion applied to change the direction of the rotor axis).

PRECESSION (the resulting angular change of the spin axis when torque is applied).

3.4 Error of gyro

Source of error is mechanical drift a directional error in a gyro is produced by random inaccuracies caused by mechanical drift and the effect of the Earth's rotation (apparent drift).

3.4.1 Three General Sources of Mechanical Drift

- Unbalance. A gyro often becomes dynamically unbalanced when operated at a speed or temperature other than that for which it was designed. The static balance of the gyro is upset when its center of gravity is not at the intersection of the three major axes. Some unbalance of both types will exist in any gyro since manufacturing processes cannot produce a perfectly balanced gyro.
- Bearing friction. Friction in the gimbals bearings results in loss of energy and incorrect gimbals positions. Friction in the rotor bearings causes mechanical drift only if the friction is not symmetrical. An

even amount of friction all around in a rotor bearing results only in a change of the speed of rotation.

- Inertia of gimbals. Energy is lost whenever a gimbals rotates because of the inertia of the gimbals. The greater the mass of the gimbals, the greater the drift from this source.

The complete elimination of mechanical drift in gyros appears to be impossibility. However, by proper design it has been kept to a minimum. Any error that still exists can be corrected for.

3.5 Disadvantages of mechanical gyro

- has mechanical error (friction moment, weight, complicated design)
- drift due earth rotation
- high cost , high weight, complicated maintenance
- cannot be integrated in electronic system and many sensors .

Chapter Four

Chapter Four

Surface acoustic wave

4.1 Surface Acoustic Wave Sensor Definition

A surface acoustic wave (SAW) is a type of mechanical wave motion which travels along the surface of a solid material. Acoustic wave (AW) devices have received increasing interest in recent years in a wide range of applications where they are currently used as resonators, filters, sensors and actuators.

SAW sensors are a class of micro-electromechanical system (MEMS) which rely on the modulation of surface acoustic waves to sense a physical phenomenon. The sensor transduces an input electrical signal into a mechanical wave which, unlike an electrical signal, can be easily influenced by physical phenomena. The device then transduces this wave back into an electrical signal. Changes in amplitude, phase, frequency, or time-delay between the input and output electrical signals can be used to measure the presence of the desired phenomenon [3].

For many MEMS structures having small amplitude oscillations, the assumption of a rigid structure simplifies the model to a one degree of freedom spring-mass-damper. This assumption leads to analytical solutions when the linearization is applied to the Reynolds equation showed below.

mean velocity is obtained by integrating the velocity distribution, across the gap:

$$u = \frac{1}{2\mu} \frac{\partial p}{\partial x} (y^2 - Hy) + u_p \left(1 - \frac{y}{H}\right) \quad (4-1)$$

indicates that the mean velocity in the gap will increase with either the plate velocity or the pressure gradient

$$u_m = -\frac{\partial p}{\partial x} \frac{H^2}{12\mu} + \frac{u_p}{2} \quad (4-2)$$

it is one form of the Reynolds equation for lubrication problems. Given an arbitrary description of the gap height as a function of position and time and boundary conditions for the pressure, it is possible to solve either analytically or numerically in order to obtain the pressure variation. The pressure distribution coupled with above equation provides the velocity distribution.

$$\frac{\partial}{\partial x} \left(\frac{\partial p}{\partial x} H^3 \right) = 6\mu u_p \frac{\partial H}{\partial x} + 12\mu \frac{\partial H}{\partial t} \quad (4-3)$$

Surface acoustic waves were discovered in 1885 by Lord Rayleigh, The first SAW device was actually made in 1965 by White and Voltmeter. They found out how to launch a SAW in a piezoelectric substrate by an electrical signal. Starting around the year 1970, SAW devices were developed for pulse compression radar, oscillators, and band pass filters for TV sets and professional radio.

In the 1980s the rise of mobile radio, particularly for cellular telephones, caused a dramatic increase in demand for filters.

The high-performance SAW filters emerged and vast numbers are now produced, around 3 billion annually.

Surface acoustic wave (SAW) sensors are used for identification and measuring of physical quantities such as temperature, pressure, torque, acceleration, tire-road friction, humidity, etc. They do not need additional power supply for the sensor elements and may be accessed wirelessly, enabling the use in harsh indoor/outdoor environments as shown in figure (4.1).

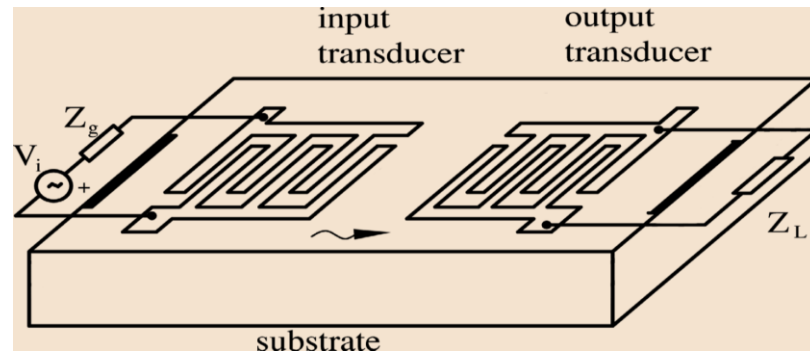


Figure3 (4.1)

the basic structure of a SAW device.

4.2 SAW types

There is two type of surface acoustic wave (SAW) the first type is Delay line and the second is Resonators. In the Delay line type the basic surface acoustic wave device consists of a piezoelectric substrate, an input interdigitated transducer (IDT) on one side of the surface of the substrate, and a second, output interdigitated transducer on the other side of the substrate. The space between the IDTs, across which the surface acoustic wave will propagate, is known as the delay-line. This region is called the delay line because the signal, which is a mechanical wave at this point, moves much slower than its electromagnetic form, thus causing an appreciable delay. . The delay line type will be discussed in details and will be used throughout this work

The interdigital transducer consists of a series of interleaved electrodes made of a metal film deposited on a piezoelectric substrate. The width of the electrodes usually equals the width of the inter-electrode gaps giving the maximal conversion of electrical to mechanical signal and vice versa. Figure (4.2) below shows DELAY LINE SAW Sensor

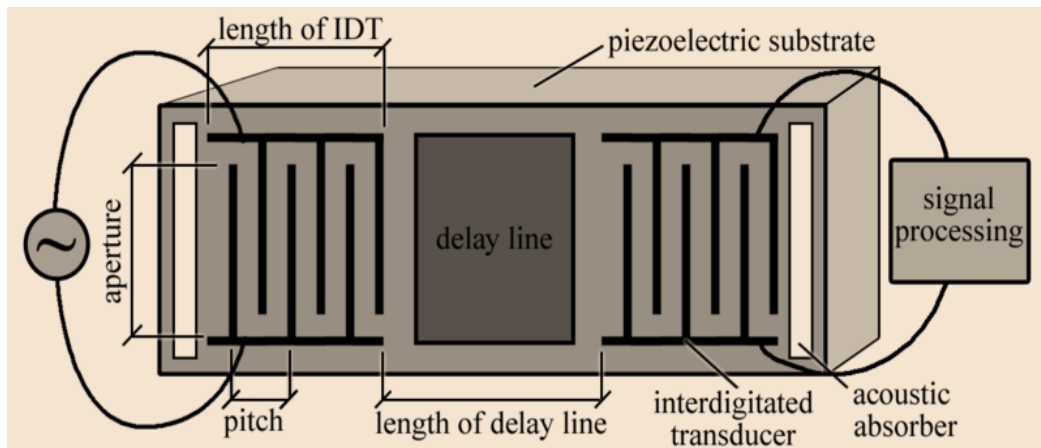


Figure (4.2)
delay line saw sensor

In the second type of SAW devices – SAW resonators, IDTs are only used as converters of electrical to mechanical signals, and vice versa, but the amplitude and phase characteristics are obtained in different ways. In resonators, the reflections of the wave from either metal stripes or grooves of small depths are used

In the one-port SAW resonator only one IDT, placed in the center of the substrate, is used for both, input and output, transductions. The input electrical signal connected to IDT, via antenna or directly, forms a mechanical wave in the piezoelectric substrate which travels along the surface on both sides from the transducer. The wave reflects from the reflective array and travels back to the transducer, which transforms it back to the electrical signal. Figure (4.3) below shows one port SAW resonator

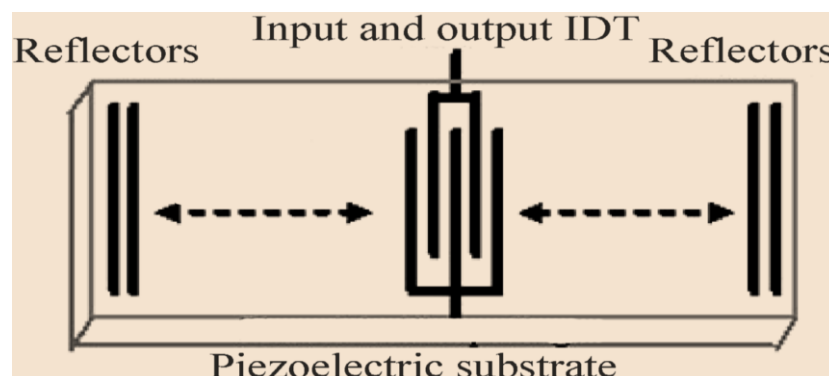


Figure5 (4.3)
One-port SAW resonator

4.3 Operation

Surface acoustic wave technology takes advantage of the piezoelectric effect in its operation. Most modern surface acoustic wave sensors use an input interdigitated transducer (IDT) to convert an electrical signal into an acoustic wave.

The sinusoidal electrical input signal creates alternating polarity between the fingers of the interdigitated transducer. Between two adjacent sets of fingers, polarity of the fingers will be switched (e.g. + - +). As a result, the direction of the electric field between two fingers will alternate between adjacent sets of fingers. This creates alternating regions of tensile and compressive strain between fingers of the electrode by the piezoelectric effect, producing a mechanical wave at the surface known as a surface acoustic wave. As fingers on the same side of the device will be at the same level of compression or tension, the space between them 'known as the pitch' is the wavelength of the mechanical wave. We can express the synchronous frequency f_0 of the device with phase velocity v_p and pitch p as:

$$f_0 = \frac{v_p}{p} \quad (4-4)$$

The synchronous frequency is the natural frequency as which mechanical waves should propagate. Ideally, the input electric signal should be at the synchronous frequency to minimize insertion loss.

As the mechanical wave will propagate in both directions from the input IDT, half of the energy of the waveform will propagate across the delay line in the direction of the output IDT. In some devices, a mechanical absorber or reflector is added between the IDTs and the edges of the substrate to prevent interference patterns or reduce insertion losses respectively.

The acoustic wave travels across the surface of the device substrate to the other interdigitated transducer, converting the wave back into an electric signal by the piezoelectric effect. Any changes that were made to the mechanical wave will be reflected in the output electric signal. As the characteristics of the surface acoustic wave can be modified by changes in the surface properties of the device substrate, sensors can be designed to quantify any phenomenon which alters these properties.

Typically, this is accomplished by the addition of mass to the surface or changing the length of the substrate and the spacing between the fingers [4].

4.4 SAW sensors advantages

The SAW sensors have the significant advantage over traditional sensors of operating passively and requiring no local, active electronic circuits. Using active electronic circuits in a sensor limits the environmental conditions in which they can be deployed. Traditional sensors cannot tolerate wide temperature ranges, and they are susceptible to failure in high radiation environments. Active circuits increase cost, increase complexity, and can decrease reliability.

The SAW sensors are relatively inexpensive to manufacture. Because they have no moving parts and are essentially an all crystalline device, they can be varying compact and rugged. This allows their use in new applications that were not previously possible. With their low profile, no need for batteries, and wireless operation, they can even monitor every blade in a turbine engine rotating at 50,000 rpm.

Another major benefit sets this innovation apart. The SAW sensors array can monitor not only one but also many variables at the same time, within the same network. Array deployment is possible with many types of sensors, some measuring pressure, some measuring temperature, and others measuring stress or strain.

4.5 Application areas

In the last thirty years surface acoustic wave (SAW) devices have found diverse applications outside their conventional fields of application – communications and signal processing – as identification tags, chemical and biosensors, and as sensors of different physical quantities. Some of application areas will be listed below

- Aerospace

Spacecraft surfaces that experience extreme temperatures, Turbine blade real-time stress and strain detection, Vehicle acceleration force monitoring, Rotational and directional sensing, Critical pressure loss detection.

- Automotive:

- Combustion Control:

Hydrocarbons, Carbon monoxide, Nitric Oxides, Oxygen

Particulates.

- Engine Performance Control

Air/Fuel ratio, Oil quality / viscosity, Other Physical Sensors – Tire pressure, torque, and Acceleration.

- Industrial and Environmental:

- Electrical Power Generation (Coal-Fired Combustion).

- Municipal, Medical, and Low Level Nuclear Waste Incineration.

- Water Quality, Aquaculture, Coastal, Inland, Drinking Water Reserves, and Ground Water.

- Oxygen, Conductivity/Salt/pH, Chlorophyll.

- Food Industry:

Process Control, moisture Content, Viscosity and Texture, pH and Conductivity (acidity and Salt Content), sugar Content (Glucose and Sucrose), food Freshness, etc

- Medical:

Point-of-care Diagnostics, Emergency Room Diagnostics, Drug Discovery and Development, Identifying specificity of proteins with other drugs, etc

- Aviation:

- military Applications:

- Radar Pulse Compression.

- ECM Jammers.

- -ECCM

- -Direct Sequence Spread Spectrum.

- -Fast Frequency Hopping.

- -Ranging.

- consumer applications:
 - Analog Cellular.
 - Wireless LAN.
 - Digital Cordless.
 - Base Stations.
 - Telephone.
 - Personal Communication System.
 - Digital Cellular.
 - Surface failure detection (Fastener failure).

Chapter Five

Chapter Five

Design of Micro Electrical Mechanical system

The proposed design of a SAW MEMS gyroscope with an operation frequency of 80 MHz's. Figure (5.1a) shows the schematic diagram and working principle of the gyroscope. This device consists of a two-port SAW resonator with a metallic dot array within the cavity, and two SAW oscillators structured by two delay lines, in which one is used as a sensor element (SAWS) and the other is used as a reference element (SAWF).

The details of the principle in the gyroscope system are as follows: a standing wave is generated on the two-port resonator. Metallic dots at an antinode of the standing wave vibrate in the normal direction z-axis.. When the gyroscope is subjected to an angular rotation, the induced Coriolis force (equation below) acts on vibrating metallic dots, and it is proportional to the mass of the metallic dot (m), the vibration velocity of the dot(v),and the rotational velocity of the substrate(Ω).

$$F_{\text{Coriolis}} \sim 2mv \times \Omega. \quad (5-1)$$

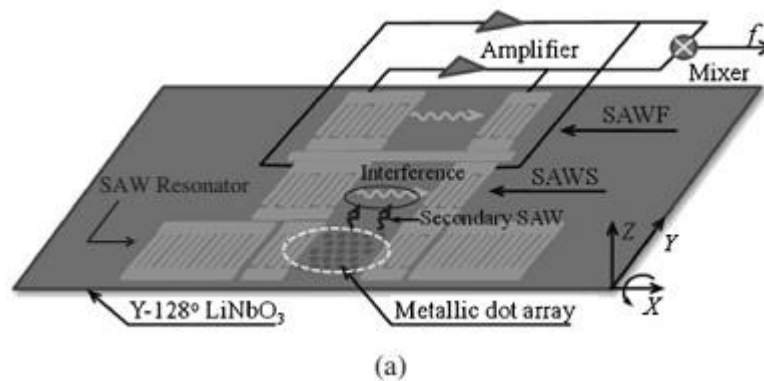


Fig6 (5.1a).

Schematic views and working principle of the SAW gyro scope Entire view of the SAW gyroscope

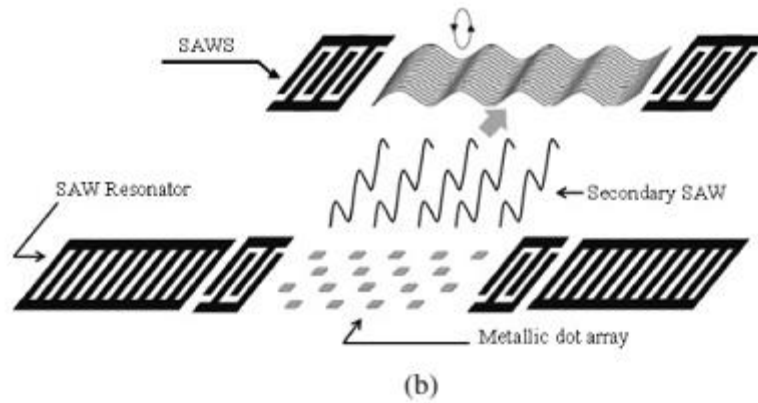


Fig7 (5.1b)

Schematic views and working principle of the SAW gyroscope working principle.

Then, the Coriolis force generates a secondary SAW in the orthogonal direction of the primary standing wave ($\pm y$ -axis). The generated secondary SAW interferes with the Rayleigh SAW propagating in SAWS, causing a change in acoustic velocity, and it induces a shift in oscillator frequency. By measuring the mixed frequency difference between the sensor oscillator and the reference oscillator, the input rotation can be evaluated.

A 128° YXLiNbO₃ is used as the piezoelectric substrate, because it has high piezoelectricity and high SAW velocity. A single-phase unidirectional transducer (SPUDT) and a comb transducer are used for the delay line design to improve the frequency stability of the oscillator. To extract optimal design parameters, the k-wave MATLAB was carried out prior to fabrication. According to the determined device parameters, the SAW gyroscope with an 80MHz operation frequency was fabricated using a standard photolithography technique. The device performance characteristics, such as sensitivity, linearity, and directivity, were evaluated. [4] [5]

5.1. Design Consideration

5.1.1 Two-port SAW resonator

A 128° YXLiNbO₃ was used as the piezoelectric substrate because it has a relatively high electromechanical coupling coefficient $K^2 = (5.56\%)$. The wave velocities of the 128° YX LiNbO₃ in the x- and y-directions are 3961 and 3656 m/s, respectively. The two-port SAW resonator was designed to generate a stable standing wave, and it is composed of input interdigital transducer (IDT), output IDT, and shorted grating reflectors, as shown in Fig (5.1a). To form a stable standing wave and to improve the resonator performance, the most critical parameter is the cavity between each shorted grating reflector and its adjacent IDT, which depends on the piezoelectric substrate, metallization, and reflector types.

In the case of the 128° YX LiNbO₃, aluminum metallization, and the shorted grating reflector type, the minimum spacing between the reflector and its adjacent IDT should be $\lambda/8$. However, this can be troublesome in high-frequency device fabrication. To overcome this fabrication limitation, and because the standing wave is periodic, both shorted grating reflectors can be moved out by an integer number of acoustic half-wavelengths. Thus, in this resonator design, the spacing was set to $5\lambda/8$. Other parameters affecting device performance are as follows:

- the number of IDT fingers
- acoustic aperture
- the number of electrodes in the shorted grating reflector.

The number of IDT finger pairs and the aperture length should be minimized to obtain good resonator performance, but there is a trade-off in choosing the aperture length because small aperture length enhances the acoustic beam diffraction. Four IDT finger pairs were chosen, and the aperture length was set to 40λ . The large spacing (50λ) between the input and output IDTs was designed for large metallic dot accommodation.

5.1.2 Metallic dot array

The role of the metallic dots is identical to that of the suspended proof mass in the micro machined gyroscope. When the gyroscope is rotated, the vibrating metallic dots at antinodes of the in-phase standing wave induce the Coriolis force, generating a secondary SAW in the orthogonal direction of its moving axis. This secondary SAW propagates towards SAWS and interferes with the Rayleigh SAW propagating in the SAWS. The sensitivity can be improved by increasing the perturbation mass weight. Depositing a thick metal with high density can increase the perturbation mass. However, excess mass loading from the metallic dots disturbs the propagation of the standing wave, resulting in a change in resonance frequency in the resonator. On the basis of our simulation analysis, 300-nm thick gold dots were used for the perturbation mass design of the gyroscope. The metallic dots were placed at the antinodes of the standing wave. The sizes of the dots were designed to be $\lambda_x/4$ and $\lambda_y/4$ to reduce the effect of the metallic dot array in the SAW resonator, where λ_x and λ_y are the wavelengths.

Along the x- and y-directions, respectively the design of the dot array was based on dot ‘‘unit cells’’, each containing two dots. The spacing (center to center) of the basic unit cells are λ_x in the x-axis and λ_y in the y-axis, as shown in Fig (5-3) the small spacing between the metallic dots and the SAWS was designed to minimize the energy loss of the secondary SAW during propagation toward the SAWS.

5.1.3 SAW delay line

The Coriolis force is determined by the mixed frequency difference between two oscillators using the SAWS and SAWF as the feedback elements. The SPUDT and combed.

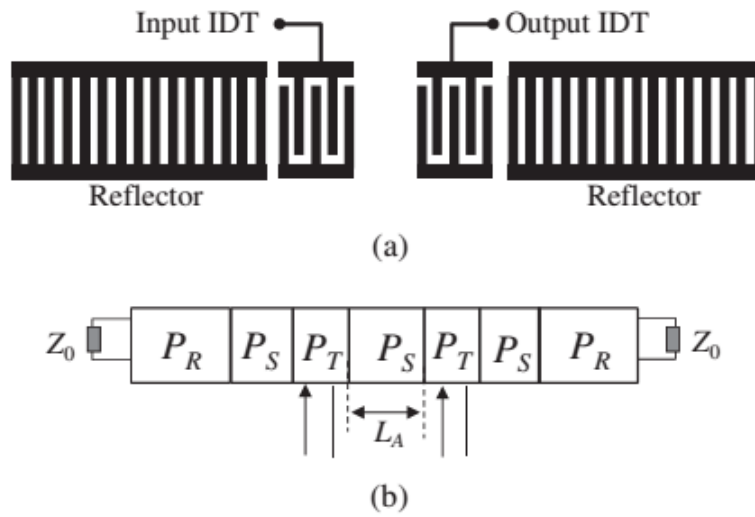


Fig 8 (5-2)

(a) Configuration of two-port SAW resonator and (b) the P matrices for the elements of the resonator

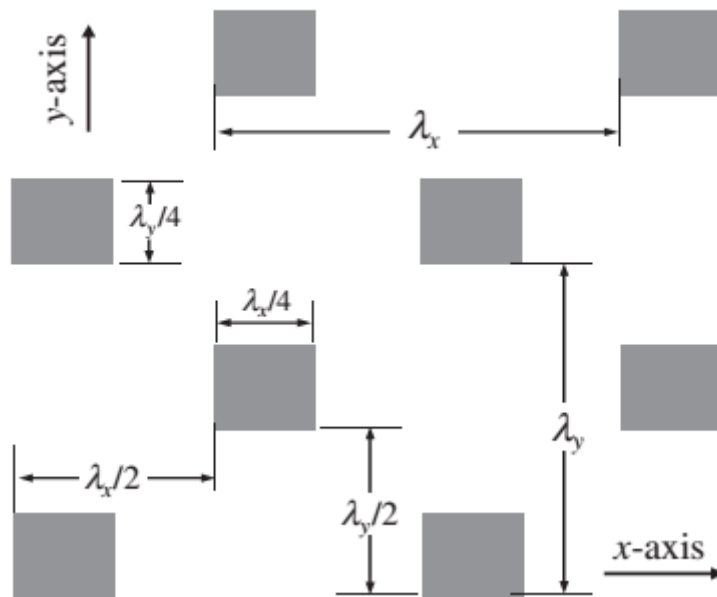


Fig 9 (5-3)

Design of metallic dot array.

5.2 k-wave Simulation

A k-wave MATLAB tool box is an efficient tool to simulate and analysis the proposed SAW gyro.

Chapter Six

Chapter Six

Simulation

This chapter includes the simulation of SAW sensor device to reach the results by using MATLAB program with the code in appendix.

6.1 Curves of response

This curve show the response of mechanical gyro .it,s very slowly

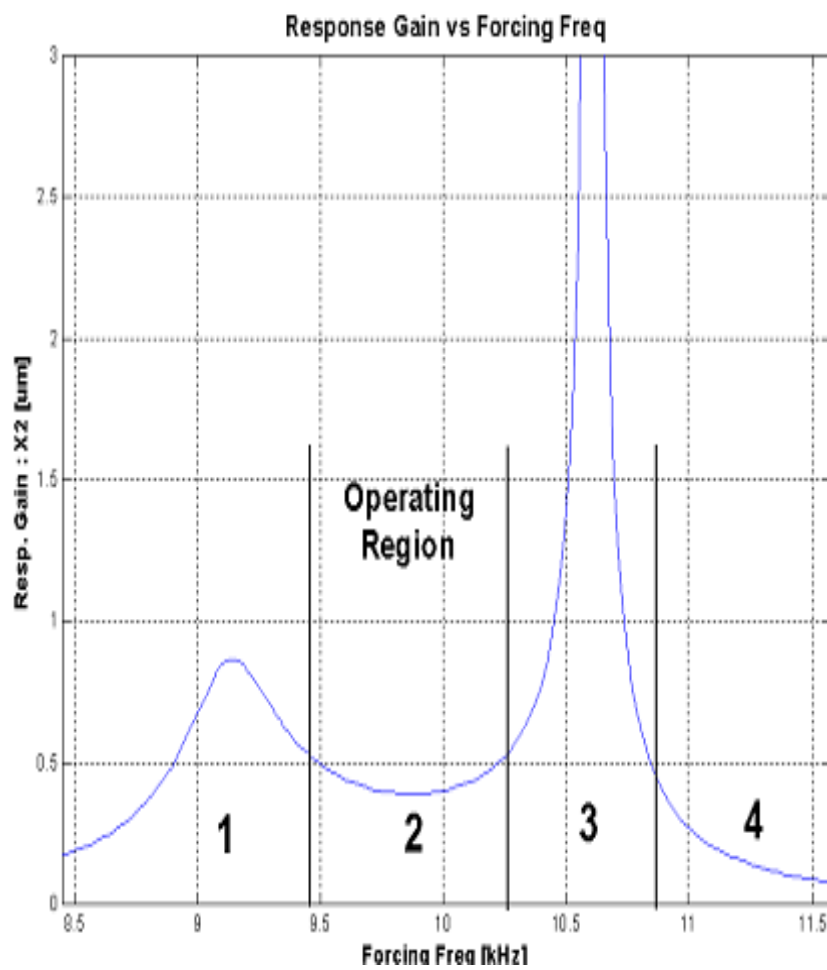
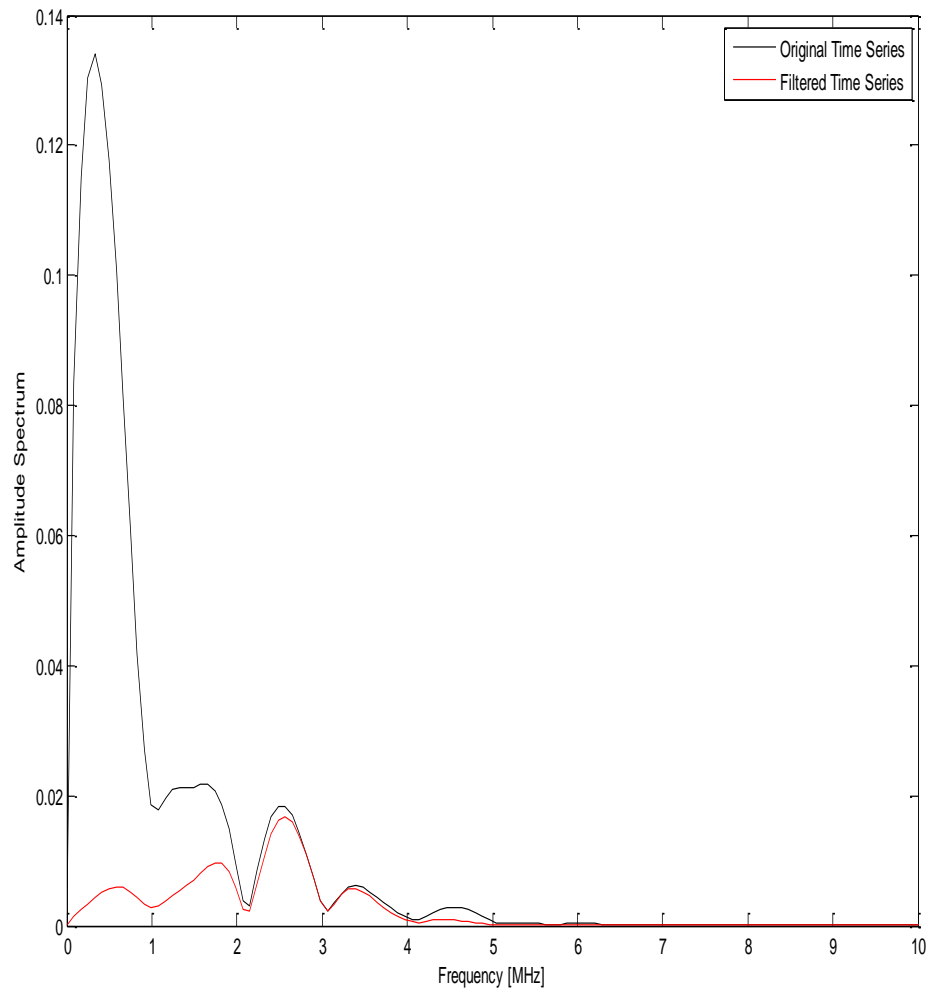


Figure10
Response of mechanical Gyro

This curve show the response of MEMS gyro .it's more faster



Figer11
Response of MEMS Gyro

Chapter Seven

Chapter Seven

Conclusion and Recommendation

7.1 Conclusion

The performance of the proposed SAW gyro is simulated and compared to a conventional gyro with same basic frequency reference. the response showed that the saw gyro has much accurate performance than the conventional one.

Once the performance carried out by simulation is acceptable then the MEMS gyro is to be chosen better than the mechanical one.

7.2 Recommendation

- We recommend that this proposed SAW gyro to be hardware realized.
- We recommended that all traditional gyro application should replace by SAW gyro.

References

References

- [1] <http://www.mnsl-journal.com/content/pdf/s40486-015-0009-z.pdf>
- [2] https://www.google.com/url?sa=t&rct=j&q=&esrc=s&source=web&cd=1&ved=0CCAQFjAAahUKEwjQk5SWxNnIAhUIXB4KHVVwDn8&url=http%3A%2F%2Fwww.wpi.edu%2FPubs%2FE-project%2FAvailable%2FE-project-042407-183027%2Funrestricted%2FExploring_Inertial_Navigation_Techniques.pdf&usg=AFQjCNEe_bk9Ua-6MaHLXof_t0PfPbEnWg
- [3] G. M. A. W.C. Wilson, "Surface Acoustic Wave in a mechanical engineering," 2008.
- [4] A. C. a. W. W. Moussa Hoummady "Acoustic Wave Sensors: design, sensing mechanisms and application," 1997.
- [5] Clark, W. A., Howe, R. T., and Horowitz, R.~1996!. "Surface micro machined Z-axis vibratory rate gyroscope". Technical Digest. Solid-State Sensor and Actuator Workshop, Hilton Head Island, S.C., June 3– 6, Transducers Research Found.283287
- [6] M. Kurosawa, Y. Fukuda, and M. Takasaki: Sens. Actuators A 66 (1998) 33
- [7] K. Jose, W. Suh, P. Xavier, V. K. Varadan, and V. V. Varadan: Wave Motion 36(2002) 367 .
- [8] V. Varadan, W. Suh, and P. Xavier: Smart Mater. Struct
- [9] Maenaka, T., Konishi, K., Fujita, Y., and Maeda, M.~1995!. "Analysis of a highly sensitive silicon gyroscope with cantilever beam as vibrating mass." Digest, The Eighth IEEE Int. Conf. on Solid-State Sensors and Actuators and Eurosensors IX. June 25–29, Stockholm, Sweden, 612– 615
- [10] Frequency locking and unlocking in a femtosecond ring laser with application to intracavity phase measurements S. Diddams, B. Atherton, J.-C. Diels. Applied Physics B: Lasers and Optics Vol. 63 1996. p. 473-480
- [11] Science and Technology Perspectives: Laser Gyroscopes ñ The Revolution in Guidance and Control William Siuru Jr
<http://www.airpower.maxwell.af.mil/airchronicles/aureview/1985/mayjun/siuru.html>
- [12] A. Kourepenis et al, Performance of Small, Low-Cost Rate Sensors for Military and Commercial Applications, Charles Stark Draper Laboratory release, (1997).

[13] Design and Analysis of a Micro-gyroscope with Sol-gel Piezoelectric Plate
Smart Material Structures. 1999 Vol. 8. 212-217. He, Nguyen, Hui, Lee, Luong.

Appendices

Appendix A (equation of motion)

- 1) x', y', z' initial position of at $t = 0$
 X, y, z initial position of at $t = t$
 x' \longrightarrow Hp
 z' \longrightarrow $z : \alpha$ in vp
- 2) \bar{M} is a disturbing torque
- 3) \bar{H} is moment of momentum

$$\bar{M} = \frac{d\bar{H}}{dt} = \left(\frac{d\bar{H}}{dt}\right)_0 + \bar{\omega} \times \bar{H}$$

$\left(\frac{d\bar{H}}{dt}\right)_0$ motion of the gyro $\bar{\omega}, r, k$ system of coordinates .

$\bar{\omega} \times \bar{H}$ Motion of all coordinate system $\bar{\omega}, r, k$ space .

$$\bar{M}_x = \frac{d\bar{H}_x}{dt} + (\bar{\omega}_y H_z - \bar{\omega}_z H_y)$$

$$\bar{M}_y = \frac{d\bar{H}_y}{dt} + (\bar{\omega}_z H_x - \bar{\omega}_x H_z)$$

$$\bar{M}_z = \frac{d\bar{H}_z}{dt} + (\bar{\omega}_x H_y - \bar{\omega}_y H_x)$$

we have From the drawing

$$\omega_x = \dot{\alpha} \omega_y = \dot{\beta} \sin \alpha \quad \omega_z = \dot{\beta} \cos \alpha$$

$$\bar{H}_x = J_x \omega_x \quad \bar{H}_y = J_y \omega_{y \text{ tot}}$$

$$\bar{H}_z = J_z \omega_z$$

$$\bar{H}_y = J_y \omega_{y \text{ tot}} = J_y (\omega_s + \omega_y)$$

$$\bar{H}_x = J_x \dot{\alpha}$$

$$\bar{H}_y = J_y (\omega_s + \dot{\beta} \sin \alpha) = J_y (\dot{\psi} + \dot{\beta} \sin \alpha)$$

$$\bar{H}_z = J_z \dot{\beta} \cos \alpha$$

$$\bar{M}_x = J_x \ddot{\alpha} + J_z \dot{\beta} \cos \alpha \cdot J_z \dot{\beta} \sin \alpha - J_y (\dot{\beta} \sin \alpha + \dot{\psi}) \dot{\beta} \cos \alpha$$

$$\bar{M}_y = J_y \frac{d}{dt} (\dot{\beta} \sin \alpha + \dot{\psi}) + J_x \dot{\alpha} \dot{\beta} \cos \alpha - \dot{\beta} \dot{\alpha} \cos \alpha - J_z \dot{\beta} \dot{\alpha} \cos \alpha$$

$$\bar{M}_z = J_z \frac{d}{dt} (\dot{\beta} \cos \alpha) + J_y \dot{\alpha} \dot{\beta} \sin \alpha - \dot{\beta} \dot{\alpha} \cos \alpha + \dot{\psi} \dot{\alpha} - J_x \dot{\alpha} \dot{\beta} \sin \alpha$$

Assuming α is very small $\cos\alpha = 1$, $\sin\alpha = 0$

And

1. $\dot{\psi} \gg \dot{\beta}$, $\dot{\psi} \ll \dot{\alpha}$
2. α, β are small angles
3. *Neglect* the motion y direction

then we get :

$$\bar{M}_x = J_x \ddot{\alpha} - J_y \dot{\psi} \dot{\beta}$$

$$\bar{M}_z = J_z \ddot{\beta} + J_y \dot{\psi} \dot{\beta}$$

But $\dot{\psi} = \omega_s$ and $H = J\omega_s$

$$\therefore \bar{M}_x = J_x \ddot{\alpha} - J_y \bar{H} \dot{\beta}$$

$$\bar{M}_z = J_z \ddot{\beta} + \bar{H} \dot{\alpha} \text{ gyro technical eqns}$$

These are two simultaneous D.E of the second degree it can be solved

$$\alpha = \frac{M_x J_z}{H^2} - \frac{M_x J_z}{H^2} \cos \Omega t$$

$$\beta = \frac{-M_x}{H} t - \frac{M_x \sqrt{J_x J_z}}{H^2} \sin \Omega t$$

When $\Omega = \frac{Hz}{\sqrt{J_x J_z}}$

From Gyro technical eqns and Laplace we get :

$$M_x(s) = J_x S^2 \alpha(s) - Hs \beta(s)$$

$$M_z(s) = J_z S^2 \beta(s) - Hs \alpha(s)$$

The transfer function

$$\frac{\alpha(s)}{Mz(s)} = \frac{1}{H} \frac{\Omega^2}{\Omega^2 + s^2}$$

$$\frac{\alpha(s)}{Mx(s)} = \frac{Jz}{H^2} \frac{\Omega^2}{\Omega^2 + s^2}$$

$$\frac{\beta(s)}{Mz(s)} = \frac{Jx}{H^2} \frac{\Omega^2}{\Omega^2 + s^2}$$

$$\frac{\beta(s)}{Mx(s)} = -\frac{1}{H^2} \frac{\Omega^2}{\Omega^2 + s^2}$$

Appendix B (MATLAB Code)

Part one (the subsidiary M-file (mechanical gyro))

```
w1x=sqrt ( k1x/m1);      %res . freq . M1, drive [ rad / sec ]
w1y=sqrt ( k1y/m1);      %res . freq . M1, sense [ rad / sec ]
w2x=sqrt ( k2x/m2);      %res . freq . M2, drive [ rad / sec ]
w2y=sqrt ( k2y/m2);      %res . freq . M2, sense [ rad / sec ]
f1x =w1x /( 2*pi )/1000      %res . freq . M1, drive [ kHz ]
f1y =w1y /( 2*pi )/1000      %res . freq . M1, sense [ kHz ]
f2x =w2x /( 2*pi )/1000      %res . freq . M2, drive [ kHz ]
f2y =w2y /( 2*pi )/1000      %res . freq . M2, sense [ kHz ]

% Dual Mass System Peak Locations :-----

gamx=f2x / f1x ;

gamy=f2y / f1y ;

cflx = sqrt (( 1 / gamx ^2 +(1+ beta ) + sqrt((1/gamx ^2+(1+ beta ))^2 4 / gamx ^ 2 ) )
/ 2 );

cfhx = sqrt (( 1 / gamx ^2 +(1+ beta )  sqrt((1/gamx ^2+(1+ beta ))^2 4 / gamx ^ 2 ) )
/ 2 );

cfly = sqrt (( 1 / gamy ^2 +(1+ beta ) + sqrt((1/gamy ^2+(1+ beta ))^2 4 / gamy ^ 2 ) )
/ 2 );

cfhy =sqrt (( 1 / gamy ^2 +(1+ beta )  sqrt((1/gamy ^2+(1+ beta ))^2 4 / gamy ^ 2 ) )
/ 2 );
```

```
f-ol-x = f2x * cflx
```

```
f-oh-x = f2x * cfhx
```

```
f-ol-y = f2y * cfly;
```

```
f-oh-y = f2y * cfhy;
```

Part two (the subsidiary M-file (MEMS gyro))

```
Nx = 128;           % number of grid points in the x
                    (row) direction
Ny = 128;           % number of grid points in the y
                    (column) direction
dx = 0.1e-3;       % grid point spacing in the x
                    direction [m]
dy = 0.1e-3;       % grid point spacing in the y
                    direction [m]
kgrid = makeGrid(Nx, dx, Ny, dy);

% define the properties of the propagation medium
medium.sound_speed = 1500; % [m/s]
medium.alpha_coeff = 0.75; % [dB/(MHz^y cm)]
medium.alpha_power = 1.5;

% define the time array
[kgrid.t_array, dt] = makeTime(kgrid,
medium.sound_speed);

% create initial pressure distribution using makeDisc
disc_magnitude = 5; % [Pa]
disc_x_pos = 50;    % [grid points]
disc_y_pos = 50;    % [grid points]
disc_radius = 8;    % [grid points]
disc_1 = disc_magnitude*makeDisc(Nx, Ny, disc_x_pos,
disc_y_pos, disc_radius);
```

```

disc_magnitude = 3; % [Pa]
disc_x_pos = 80; % [grid points]
disc_y_pos = 60; % [grid points]
disc_radius = 5; % [grid points]
disc_2 = disc_magnitude*makeDisc(Nx, Ny, disc_x_pos,
disc_y_pos, disc_radius);

source.p0 = disc_1 + disc_2;

% define a centered circular sensor
sensor_radius = 4e-3; % [m]
num_sensor_points = 50;
sensor.mask = makeCartCircle(sensor_radius,
num_sensor_points);

% run the simulation
sensor_data = kspaceFirstOrder2D(kgrid, medium, source,
sensor);

% define the frequency response of the sensor elements
center_freq = 3e6; % [Hz]
bandwidth = 80; % [%]
sensor.frequency_response = [center_freq, bandwidth];

% re-run the simulation
sensor_data_filtered = kspaceFirstOrder2D(kgrid, medium,
source, sensor);

% calculate the frequency spectrum at the first sensor
element
[f, sensor_data_as] = spect(sensor_data(1, :), 1/dt);
[f, sensor_data_filtered_as] =
spect(sensor_data_filtered(1, :), 1/dt);

%
=====

% VISUALISATION

```

```
%  
=====
```

```
% plot the amplitude spectrum  
figure;  
[f_sc, scale, prefix] = scaleSI(max(f(:)));  
plot(scale*f, sensor_data_as, 'k-', scale*f,  
sensor_data_filtered_as, 'r-');  
ylabel('Amplitude Spectrum');  
xlabel(['Frequency [' prefix 'Hz]']);  
legend('Original Time Series', 'Filtered Time Series');  
set(gca, 'XLim', [0 10]);
```